

M. Xia
Centre for Advanced Materials Joining,
University of Waterloo,
Waterloo, Ontario, Canada;
Central Iron & Steel Research Institute,
Beijing, P. R. China

N. Sreenivasan

S. Lawson

Y. Zhou
e-mail: nzhou@uwaterloo.ca

Centre for Advanced Materials Joining,
University of Waterloo,
Waterloo, Ontario, Canada

Z. Tian
Central Iron & Steel Research Institute,
Beijing, P. R. China

A Comparative Study of Formability of Diode Laser Welds in DP980 and HSLA Steels

Understanding effects of welding on strength and formability is critical to support wider application of advanced high strength steels in automotive components. In this study, High Strength Low Alloy (HSLA) and DP980 (Dual Phase, 980 MPa) sheet steels were welded with a 4 kW diode laser. Mechanical properties of welds and parent metals were assessed by tensile and limiting dome height tests, and related to microhardness distribution across the welds. The formability of HSLA welds was insensitive to the welding process and comparable to that of parent metal. For the DP steel, weld formability was much lower than that of corresponding parent metal, which appeared to be due to the formation of soft zones in the outer region of the Heat affected zone (HAZ) of the welds. It was found that increase of welding speed resulted in a slight increase of formability of the DP steel, associated with a reduction in the microhardness difference between base metal and HAZ soft zones. [DOI: 10.1115/1.2744417]

Keywords: advanced high strength steel, laser welding, microhardness profile, formability

1 Introduction

In order to reduce automobile weight and to increase the fuel efficiency, manufacturers are urgently seeking new steels that combine good ductility and high strength. Many high strength steels are emerging to meet this demand, such as dual phase (DP), transformation induced plasticity, twin induced plasticity, and martensitic steels. These steels achieve their high strength through a combination of chemistry and processing, with yielding tensile strength from 340 MPa to 1500 MPa. DP steel is an emerging class of high strength steel having a microstructure of strong martensite and/or bainite colonies dispersed in a soft matrix of ferrite. DP steels are produced by intercritical annealing to create high purity ferrite and austenite, which are then rapidly cooled, so the austenite is transformed into martensite and the ferrite is retained on cooling [1]. It is well known that the DP steels have a number of desirable properties such as absence of yield point, low yield/tensile strength ratio, high work hardening rate, and high uniform elongation. The last two properties indicate the presence of excellent formability that, coupled with its high tensile strength, has made this steel attractive for weight saving applications, especially in automobile industry for greater fuel economy. However, the wide application of this kind of steel in auto industry makes weldability research and weld property evaluation an imperative job.

So far, weldability research on DP series has been focused mainly on the resistance spot welding technique [2,3]. Arc welding and flash butt welding processes for DP steel welding were also reported [4,5]. Traditional mild and HSLA steels have a reputation for unproblematic response to welding. In contrast, welds in DP steels may develop very high peak hardness [6], and especially in lower energy density welding processes such as gas metal arc welding, local soft zones are seen in the outer HAZ in most cases [4]. The diode laser as used in this study offers a promising alternative welding process for automotive component fabrication; little industrial experience has been reported so far in diode weld-

ing of steels [7]. Its beam geometry results in weld characteristics intermediate between arc welds and welds made with traditional keyholing lasers (CO₂, YAG) [8].

Formability is one of the most important mechanical characteristics in materials for auto parts. Although a formability comparison has been made between HSLA and DP steels [9], little research has been conducted on the effects of welding on formability of DP steels [10,11]. Inhomogeneity of microstructures and properties across a weld brought about by the welding process may greatly change the deformation response of a weld and thus the overall welded specimen properties. Numerous studies have so far been reported of the formability of tailor welded blanks; e.g. [7,12–14]. However, the focus of attention has almost invariably been the effects on forming of dissimilar material properties or thickness across the weldment, which has served to obscure the role of welding itself upon the deformation characteristics. Therefore, in the present work, tailored blanks for formability testing were simply created with identical material properties on each side of the joint by carrying out full-penetration bead-on-plate welding on circular blanks precut to fit the dome height testing apparatus. Comparison of the behavior of welded and unwelded blanks was thus able to focus exclusively on welding-related phenomena.

2 Experimental Procedures

The steels, i.e., HSLA and DP980, employed in this study were deliberately chosen to explore potential effects on deformation behavior of the increased carbon and alloy contents and resultant hardenability behavior of the new DP steels. The microstructures of DP and HSLA sheet materials used in this work are shown in Fig. 1. The DP steel has a ferrite matrix with a significant volume fraction of fine martensite grains. The HSLA steel also has a fine-grained ferrite matrix with very small dispersed colonies of alloy carbides. A summary of compositional data and mechanical properties is provided in Tables 1 and 2.

A Nuvonyx ISL4000L diode laser operating at 4 kW was used to weld all specimens, with welding speed varying from 1.0 m/min to 1.6 m/min. With the relatively large rectangular focal spot provided by this laser (0.5 × 12 mm), 1.6 m/min was the maximum travel speed at which fully penetrated welds with

Contributed by the Materials Division of ASME for publication in the JOURNAL OF ENGINEERING MATERIALS AND TECHNOLOGY. Manuscript received June 19, 2006; final manuscript received January 4, 2007. Review conducted by Prof. Golam Newaz.

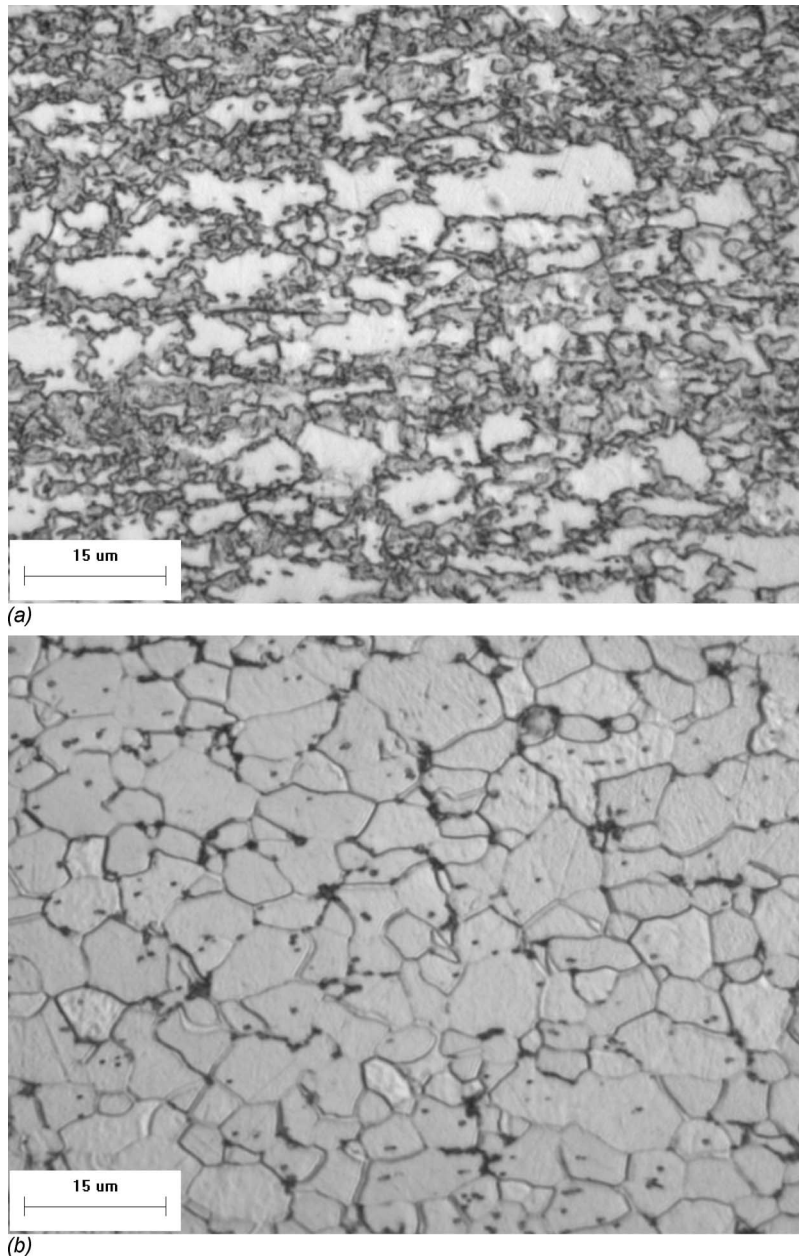


Fig. 1 Microstructures of the base metals: (a) DP980 and (b) HSLA

nearly two-dimensional heat flow could be produced. Decrease of welding speed to 1.0 m/min permitted evaluation of the effect of increased heat input (energy per unit weld length), leading to a

Table 1 Chemical compositions (wt%) of DP980 and HSLA

Steel	C	Mn	Mo	Si	Cr	Al	B
DP980	0.135	2.1	0.35	0.05	0.15	0.45	0.007
HSLA	0.056	0.64	0.015	0.026	0.09	0.06	0.00017

Table 2 Mechanical properties of DP980 and HSLA

Steel thickness (mm)	Yield strength (MPa)	Ultimate strength (MPa)	Elongation (%)	Hardness (HV)
DP980 (1.2)	534	980	12.2	283±2
HSLA (1.14)	380	470	32.1	163±4

lower post-weld cooling rate. High purity argon was applied for shielding to the top surface only, at a flow rate of 30 l/min. Base metal, fusion zone, and HAZ microstructures were evaluated using standard metallurgical techniques with samples etched with 2% nital. Vickers microhardness traverses were conducted at 500 g load on etched specimens, and linked to the observed microstructures. Tensile testing of welds was conducted both perpendicular and parallel to the weld axis at room temperature. Specimen geometry was similar to a half-size ASTM E8 sheet metal coupon, as shown in Fig. 2.

The formability of the bead-on-plate welded specimens and parent metals was evaluated using a standard limiting dome height (LDH) test apparatus with 102 mm die hemispherical punch and locked/crimped specimen edges. The formability testing apparatus is shown schematically in Fig. 3. To encourage essentially biaxial, pure stretching deformation, all formability test coupons were fully circular, without cutouts. In the present work, sheets were lightly coated with mill oil before testing.

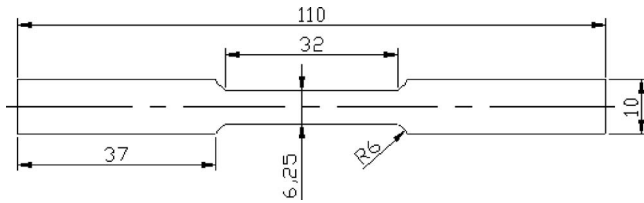


Fig. 2 Schematic diagram of tensile test coupons

3 Results

3.1 Weld Microstructure and Hardness. Representative hardness profiles across the welds in both steels are presented in Fig. 4. In both steels, the hardness profile was relatively flat across the weld metal itself, with the DP steel showing a very high hardness in the fusion zone and high-temperature HAZ, as could be expected from its chemistry. The microstructure of the DP steel fusion zone was thought to be mainly comprised of martensite as shown in Fig. 5(a), and moreover the hardness was close to levels generally associated with a fully martensite product [15]. The HSLA steel weld metal mostly consisted of ferrite sideplate and bainitic structures, as shown in Fig. 5(b). In both steels, hardness showed a progressive decrease in local hardness moving outwards through the HAZ; i.e., with lower peak temperature experienced in the weld thermal cycle. With HSLA steel, the HAZ hardness pattern merged smoothly into the unaffected base metal. As for DP steel, however, hardness “valleys” were invariably seen in the outer part of the HAZ, in which the hardness locally dropped significantly below the base metal hardness. Such valleys have previously been seen in HAZs of other DP steels [2,4,16], and were attributed to local tempering of the martensite phase of the as-manufactured steel. Microstructural examination of the HAZ showed that martensite in the base metal had decomposed to form visible carbides in a band at the outer edge of visible effects of welding in Fig. 5(c). This zone coincided with the microhardness valleys, thus confirming that the hardness reduction was directly related to tempering.

While fusion zone hardness and microstructure were not strongly affected by welding speed (which affects the shape of the thermal cycle caused by the welding operation), welding speed did have a significant effect on the HAZ soft zone, affecting the location and width of the soft zone, and the minimum hardness, which can be observed in Fig. 4(b) and Table 3. Generally speaking, with the increase of the welding speed, in other words, with the decrease of heat input, the width and depth of softening were both reduced.

3.2 Tensile Testing. Uniaxial tensile testing, longitudinally and transversely, was used to characterize weld deformation and

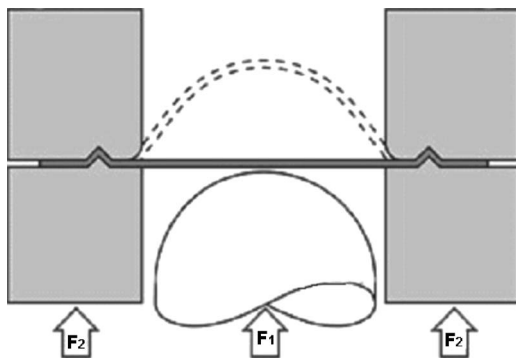
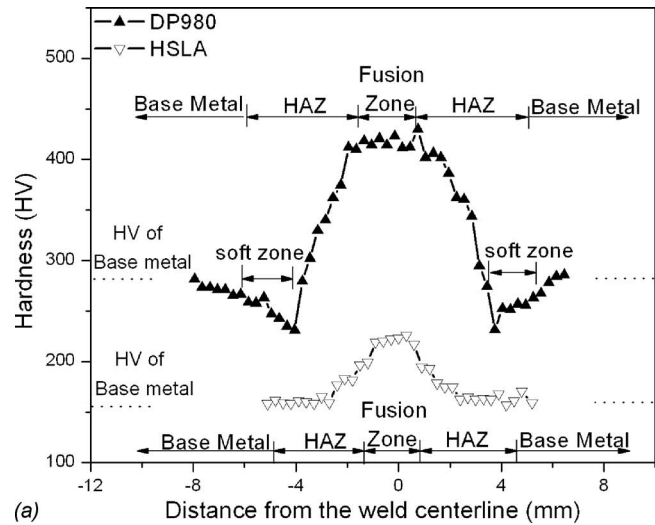
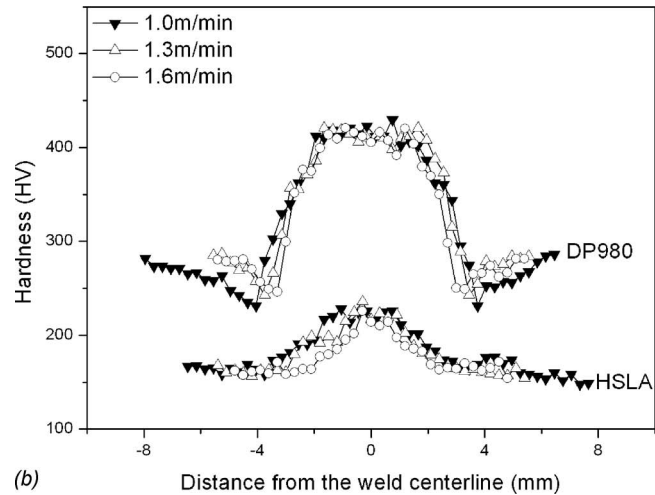


Fig. 3 Schematic graph showing tooling and specimens for the limiting dome height test. Specimen after increase of deformation shown as dotted lines.



(a) Hardness profiles of DP980 and HSLA at welding speed of 1.0 m/min

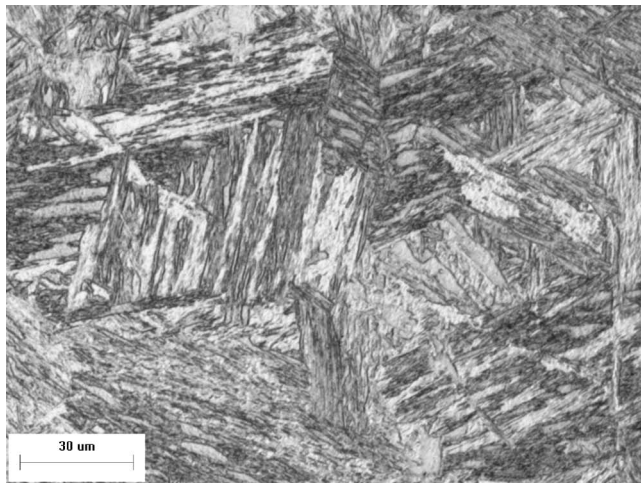


(b) Hardness profiles of DP980 and HSLA welds with different welding speeds

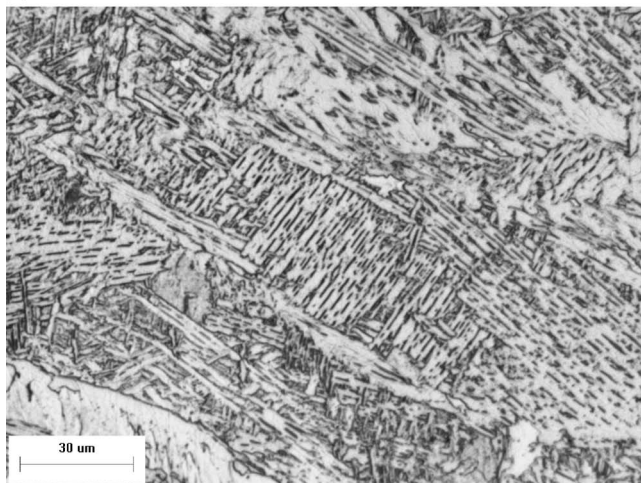
Fig. 4 Hardness profiles of (a) DP980 and HSLA at welding speed of 1.0 m/min; (b) DP980 and HSLA welds with different welding speeds; locations and dimensions of the soft zone were listed in Table 3

failure modes and to evaluate the strength of welds. The testing results are shown in Figs. 6 and 7. Transverse tensile tests of DP welds showed ultimate tensile strength lower in all cases than the base metal (Fig. 6). Furthermore, failure occurred by ductile rupture in the outer HAZ, exactly at the location of the hardness valley (Fig. 7(a)). Examination of the deformation pattern along the transverse specimens showed that yielding occurred first in the soft zones and much of the total plastic strain was concentrated there. This led in turn to a reduction in overall specimen elongation, as necking and failure occurred in the HAZ before the balance of the specimen was fully work-hardened.

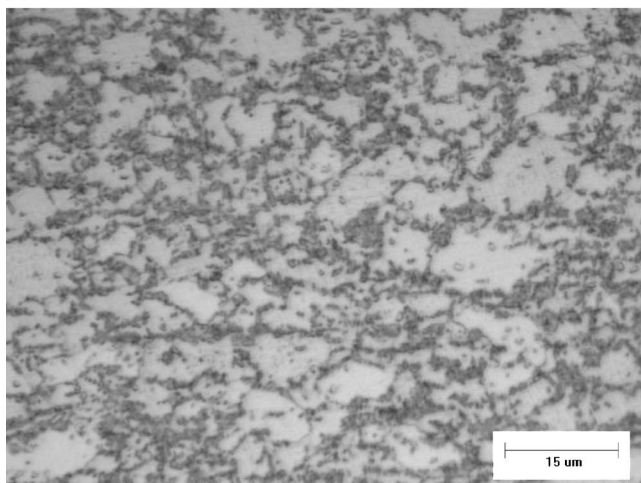
In tensile tests parallel to the weld axis, all weld zones are forced to strain equally, and zones of different local hardness/strength contribute in parallel to overall load-bearing capacity. All specimens showed strength in excess of the base metal, which would be expected as the fusion zone and most of the HAZ was harder than the base metal. The fracture site in longitudinal tests was randomly distributed as shown in Fig. 7(b). Interpretation of strength data from longitudinal tests is complex because each specimen is a composite of various layers having varying flow properties, including the fusion zone, continuous gradations of properties in the HAZs on both sides of the weld, plus a thickness of unaffected base metal dependent on fusion zone width in relation to specimen width. Actual strength data obtained were found



(a)



(b)



(c)

Fig. 5 Fusion zone microstructure of (a) DP980 and (b) HSLA welds. (c) Soft zone microstructure DP980 weld, showing martensite tempering.

in each case to reasonably reflect a weighted sum of the widths of constituents present and their local flow properties based on correlation with local hardness. Recognizing the difficulties of interpreting strength data from longitudinal tensile test, these tests were included in the investigation mainly to verify that significant embrittlement was not being included in any weld zone(s) by the

Table 3 The influence of the welding speed on the soft zone of DP980 steel

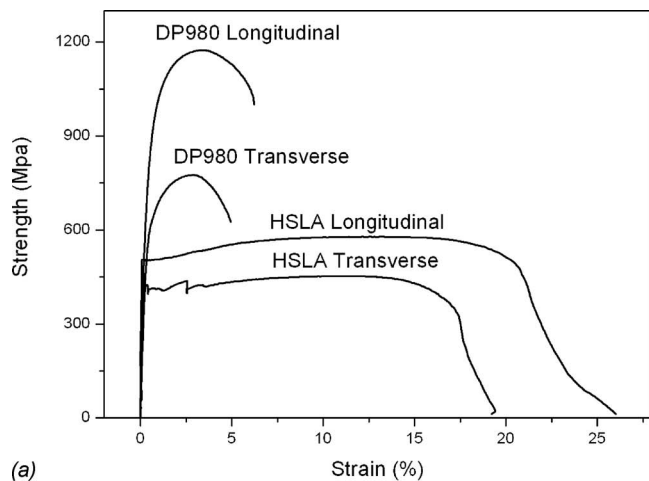
Welding speed (m/min)	Distance of the soft zone ^a (mm)	Width of the soft zone ^b (mm)	Minimum hardness across the weld (HV)
1.0	4.12	1.50	228
1.3	4.05	1.40	231
1.6	3.30	0.90	246

^aThe distance of the soft zone refers to the distance between minimum hardness location and the weld center.

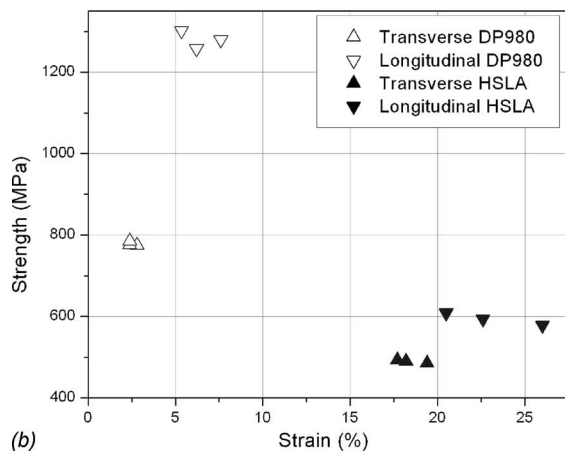
^bWidth of the soft zone is the average width of soft zones on both sides of the hardness profiles.

welding process. However, all welded longitudinal and transverse specimens showed significant amounts of plastic strain, in spite of the higher weld metal hardness than the base metal; the HSLA welds showed excellent elongation.

3.3 Formability Testing. Top views of representative tested specimens are shown in Fig. 8, after dome height testing to the point of coupon rupture. Figures 8(a), 8(b), and 8(e) are DP980 and HSLA parent metal specimens, whereas Figs. 8(c), 8(d), and 8(f) are tests of welded blanks. In DP parent steel, fracture path was at a radial distance of about 17 mm from the disk center and



(a)



(b)

Fig. 6 Stress-strain data on both steels. (a) Typical stress-strain curves for DP980 and HSLA transverse and longitudinal tests with the welding speed of 1.3 m/min. (b) Ultimate strength versus ultimate strain of HSLA and DP980 weldment with three welding speeds.

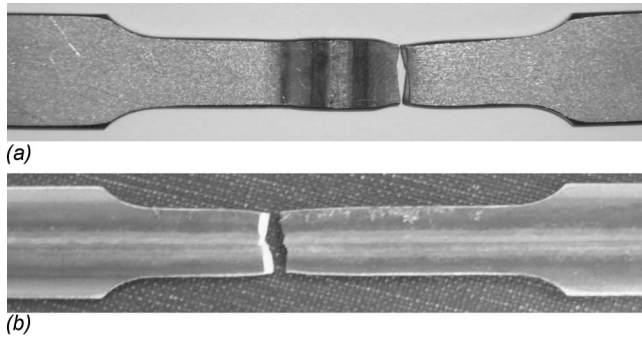


Fig. 7 Typical tensile tested DP welded specimens: (a) Transverse and (b) longitudinal

propagated in a direction parallel to the rolling directions in all tests (Fig. 8(b)). Thus, this DP steel displayed strong directionality in terms of formability. The fracture path in dome height testing of HSLA parent metal differed significantly from that in the DP steel. The crack followed a curved, arc path, and the radial distance from the fracture path to disk center was about 30 mm (Fig. 8(e)).

Fractures of laser welded specimens of both steels in LDH test followed fundamentally different paths. In the DP welded specimens, the fracture path was always entirely in the outer HAZ, at a radial distance of about 4 mm from the weld centerline, regardless of welding directions (whether parallel or perpendicular to the rolling direction) (Fig. 8(d)). The welded specimens' LDH strain at failure was much lower than that of the corresponding parent metal, which indicates that in this material, the formability property was significantly reduced by welding. The formability degradation was also demonstrated by the big gap of dome height in Fig. 9(a). As for HSLA welded specimens, no significant difference in fracture path was observed between welded specimens and parent metal. The minimum radial distance from the dome apex to the fracture path was essentially the same in base metal and welded coupons and both exhibited an oblique curved fracture feature as shown in Figs. 8(e) and 8(f). Such high consistency implied that, unlike the case of DP steel, the welding process had no significant influence on the formability properties of HSLA. This is also consistent with the fracture height results in Fig. 9(b), where strains in base metal and welded coupons were essentially equal.

4 Discussion

In uniaxial tensile testing of DP welded specimens, the fracture coincided with the soft zone. In the formability test, full-circle biaxially loaded specimens were used, which tended to impose the same overall strain conditions in all radial directions. The distribution of the strain in the LDH test is related both to the work-hardening behavior and to friction conditions [17]. In addition, parent metal specimens of two experimental steels could be considered uniform in terms of microstructures and mechanical properties. When the parent metal with centrosymmetry underwent LDH testing, the fracture could be considered to happen at the sites where actual local strain first exceeded the material's maximum strain capacity for that orientation. It could be inferred that the maximum strain sites for the DP parent steel and HSLA parent steel in the formability test were positions at which the radial distances from the center were about 17 mm and 30 mm, respectively. The above formability difference of two parent metals can be explained as follows. In LDH testing of homogeneous materials, the strain intensity at the dome apex is normally relatively low, and the greatest strain intensity and usual failure location is usually seen in an annular band whose radius depends on the strain-hardening behavior of the material and on the friction conditions between sheet and punch. Under the same friction conditions, the higher strain hardening n -value of DP steel than HSLA

means that the former will show bigger maximum strain intensity. In this connection, failure at a smaller radial distance from the center was observed for higher n -value DP steels [18].

In DP steel, the greatly different fracture path between parent metal and welded specimens served to emphasize the negative influence of welding process on formability, as also shown by the big difference in maximum height before failure in Fig. 9(a). Rupture occurred invariably at the soft zone in DP welded steel, which was previously identified by hardness testing and uniaxial tensile testing. Thus, in this work, the soft zone was the vulnerable region and effectively controlled the behavior in formability testing.

Association of LDH failure with welds has previously been observed in CO₂ laser-welded DP steel [10], with a tensile strength about 800 MPa. However, in that work the position of failure was in the weld and no soft zone was reported. In the present work, the fracture propagated along the soft zone, irrespective of the rolling direction. This behavior contrasts significantly with the HSLA steel formability tests, where no difference in fracture characteristics were observed between welded specimens and parent metal (Figs. 8(c) and 8(d)), and both exhibited an oblique curved fracture feature.

The simplest measure of formability is the height of the dome that can be made before the specimen fractures. The ability to stretch could be defined as the height of the dome height H divided by the diameter of punch d [19]. In order to compare the stretchability of different materials and their welded specimens under different welding conditions. The stretchability (s) is represented as follows:

$$s = \frac{H_w}{H_b} \times 100\%$$

where H_w is the dome height of the weld specimen in LDH testing (mm), and H_b is the dome height of the base metal in LDH testing (mm).

Based on the discussion above, it could be expected that the degradation of the DP welded specimen's formability may have a close relationship with the characteristics/dimensions of the soft zone in the HAZ. The stretchability-microhardness graph of DP welded specimens is plotted in Fig. 10.

It can be observed that the welded specimens with lower microhardness difference between soft zone and base metal possessed a slightly higher formability. The negative impact of the soft zone on formability could be explained as follows. In dome height testing, a larger microhardness difference implies a larger difference in plastic deformation. The soft zone deforms first and much more than the harder surroundings. In other words, the soft zone possesses lower strength than the parent metal and fusion zone, leading to a severe concentration of strain in this region. Uneven strain distribution therefore occurred, and the degree of unevenness would be expected to be more severe with a greater amount of local softening. Thus, specimens with local soft zone would show failure taking place earlier, yielding a lower average strain value and lower height consequently. Furthermore, the formation of hard martensite phase in the weld metal could aggravate the nonuniform deformation across the weld. The stretchability of welded specimens has been previously related to the hardness difference between the hardened fusion zone and base metal [19], but not to that between soft zone and base metal.

On the other hand, the HSLA welded specimens, having no soft zones in the HAZ and partly due to unremarkable hardness difference between weld and base metal, possessed excellent stretchability after welding, about 98% of base metal value.

5 Conclusions

- (1) With the diode laser welding process, a combination of severe local hardening and local softening happened across welds in DP980 steel, as a result of metallurgical change caused by the welding thermal cycle. The size of soft zones



Fig. 8 Dome tested specimens. (a) Parent metal of DP980. (b) Details of crack in (a). (c) Welded specimen of DP980 at welding speed of 1.3 m/min. (d) Details of crack in (c). (e) Parent metal of HSLA. (f) Welded specimen of HSLA.



Fig. 9 Side views of dome tested samples. The dome heights of the parent metal and welded specimen are 30.4 and 13.2 mm for DP980 (a), and 32.5 and 31.8 mm for HSLA (b). Welding speed is 1.6 m/min and welding direction is parallel to the rolling direction.

in the DP steel was related to the welding speed, being smaller at higher speeds which generated a shorter thermal cycle.

- (2) In uniaxial tensile testing, DP980 showed a sharp decrease in strain after welding, particularly in the transverse orientation. The fracture site was invariably at the soft zone in DP steel welds in transverse orientation. The HSLA weld steel also exhibited lower strain than parent metal, but enjoyed a higher strain than DP980 weld under same welding conditions.
- (3) Compared to the parent metal, sharp decrease of formability was observed for DP980 welded specimens, also influenced by the welding speed to some degree, while HSLA welded specimens possessed the same formability as parent

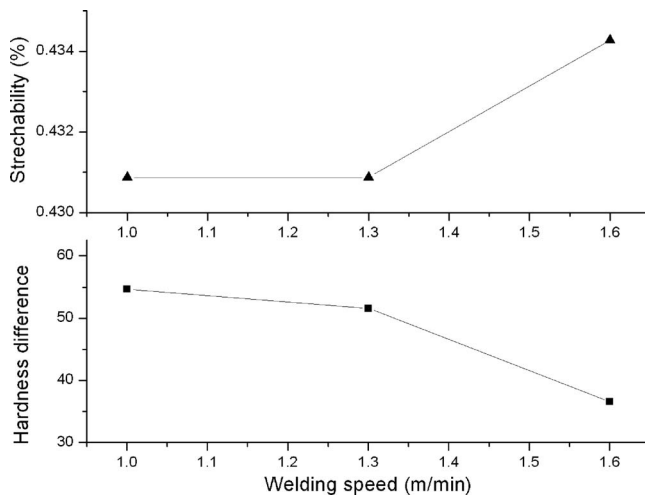


Fig. 10 The stretchability and hardness difference as a function of welding speed (welding direction parallel to the rolling direction)

metal, regardless of the welding speed. HSLA and DP steel show different sensitivities to diode laser welding in terms of formability.

- (4) The hardness distribution across the weld can be a useful indicator for the formability of laser welded sheet metals. Soft zone across the weld is detrimental to the welded specimens' formability.

Acknowledgment

This work was supported by Auto21 (www.auto21.ca), Dofasco, Huys Industries Ltd., Centerline Ltd., and International Lead Zinc Research Organization (USA).

References

- [1] Bleck, W., 1996, "Cold-Rolled, High-Strength Steels for Auto Applications," *J. Met.*, **48**, pp. 26–30.
- [2] Ghosh, P. K., Gupta, P. C., Avtar, R., and Jha, B. K., 1990, "Resistance Spot Weldability of Comparatively Thick C-Mn-Cr-Mo Dual Phase Steel Sheet," *ISIJ Int.*, **30**, pp. 233–240.
- [3] Ghosh, P. K., Gupta, P. C., Avtar, R., and Jha, B. K., 1991, "Weldability of Intercritical Annealed Dual-Phase Steel with the Resistance Spot Welding Process," *Weld. J. (Miami, FL, U.S.)*, **70**, pp. 7–s–14–s.
- [4] Hsu, C., Soltis, P., Carroscia, M., Barton, D., and Occhialini, C., 2004, "Weldability of Dual-Phase Steel with Arc Welding Processes," *Sheet Metal Welding Conference*, XI, Sterling Heights, MI, May 11–14, pp. 1–11.
- [5] Taka, T., Kunishige, K., Yamauchi, N., and Nagao, N., 1989, "Hot-Rolled Steel Sheet with Excellent Flash Weldability for Automotive Wheel Rim Use," *ISIJ Int.*, **29**, pp. 503–510.
- [6] Marya, M., and Gayden, X. Q., 2005, "Development of Requirements for Resistance Spot Welding Dual-Phase (DP600) Steels Part I—The Causes of Interfacial Fracture," *Weld. J. (Miami, FL, U.S.)*, **84**, pp. 172–s–182–s.
- [7] Bocos, J. L., Zubiri, F., Garcíandía, F., Peña, J., Cortiella, A., Berrueta, J. M., and Zapirain, F., 2005, "Application of the Diode Laser to Welding on Tailored Blanks," *Weld. Int.*, **19**, pp. 539–543.
- [8] Walsh, C. A., Bhadeshia, H. K. D. H., Lau, A., Matthias, B., Oesterlein, R., and Drechsel, J., 2003, "Characteristics of High-Power Diode-Laser Welds for Industrial Assembly," *J. Laser Appl.*, **15**, pp. 68–76.
- [9] Shi, M. F., Thomas, G. H., Chen, X. M., and Fokete, J. R., 2001, "Formability Performance Comparisons Between Dual Phase and HSLA Steels," *Proc. Symposium 43rd Mechanical Working and Steel Processing Conference, Iron & Steel Society*.
- [10] Dry, D., Waddell, W., and Owen, D. R. J., 2002, "Determination of Laser Weld Properties for Finite Element Analysis of Laser Welded Tailored Blanks," *Sci. Technol. Weld. Joining*, **17**, pp. 11–18.
- [11] Howard, K. L., 2005, "Diode Laser Welding of Aluminum Sheet," Master's thesis, University of Waterloo.
- [12] Saunders, F. I., and Wagoner, R. H., 1996, "Forming of Tailor-Welded Blanks," *Metall. Mater. Trans. A*, **127**, pp. 2605–2616.
- [13] Chan, L. C., Chan, S. M., Cheng, C. H., and Lee, T. C., 2005, "Formability and Weld Zone Analysis of Tailor-Welded Blanks for Various Thickness Ratios," *ASME J. Eng. Mater. Technol.*, **127**, pp. 179–185.
- [14] Chan, L. C., Chan, S. M., Cheng, C. H., and Lee, T. C., 2005, "Formability Analysis of Tailor-Welded Blanks of Different Thickness," *ASME J. Eng. Mater. Technol.*, **127**, pp. 743–751.
- [15] Yurioka, N., Okumura, M., and Kasuya, T., 1987, "Prediction of HAZ Hardness of Transformable Steels," *Met. Constr.*, **17**, pp. 217R–223R.
- [16] Biro, E., and Lee, A., 2004, "Welding Properties of Various DP600 Chemistries," *Sheet Metal Welding Conference XI*, Sterling Heights, MI, May 11–14, pp. 1–11.
- [17] Kalpakjian, S., 1997, *Manufacturing Processes for Engineering Materials*, 3rd ed., Addison-Wesley, Reading, MA, pp. 436–445.
- [18] Keeler, S. P., 1975, "Relationship between Laboratory Material Characterization and Press-Shop Formability," *Proceedings of Microalloying*, New York, pp. 517–527.
- [19] <http://www.msm.cam.ac.uk/phase-trans/2005/LINK/64.pdf>